This is the peer reviewd version of the followng article:

Alluvial sand composition as a tool to unravel the Late Quaternary sedimentation of the Modena Plain, northern Italy / Lugli, Stefano; Marchetti Dori, Simona; Fontana, Daniela. - STAMPA. - 420:(2007), pp. 57-72. [10.1130/2006.2420(05)]

Geological Society of America

Terms of use:

The terms and conditions for the reuse of this version of the manuscript are specified in the publishing policy. For all terms of use and more information see the publisher's website.

25/04/2024 10:27

(Article begins on next page)

Alluvial sand composition as a tool to unravel the Late Quaternary sedimentation of the Modena plain, northern Italy

Lugli Stefano, Marchetti Dori Simona and Fontana Daniela
Dipartimento di Scienze della Terra, Università degli Studi di Modena e Reggio Emilia, Largo S.Eufemia n. 19, 41100 Modena, Italy

ABSTRACT

The Modena alluvial plain is located at the northern side of the Northern Apennines thrust- and fold-belt, where streams draining the chain flow toward the north-east into the Po River. The alluvial plain is characterized by a spectacular abundance of archaeological sites of various ages and can be considered a natural laboratory for the reconstruction of the recent sedimentary evolution of the Po Plain. Detailed modal analyses of modern sands of the Modena Plain streams indicate that the provenance signal can be distinguished on the basis of key components, such as quartz, feldspar, carbonate and lithic fragments. The compositional fields of the streams depend on the extent of the watershed, the recycling of older fluvial sediments and the sediment input from tributary streams.

The modal analyses demonstrate that sand composition of the major rivers (Panaro and Secchia) has not changed during the Holocene, when sediment production, storage and dispersal were probably dominated by colluvial aggradation in an environment characterized by a dense vegetation cover.

In the Late Pleistocene, fluvial sands were characterized by higher feldspar contents compared with modern and Holocene sands. This feldspar abundance could reflect a high-frequency signal in sediment supply rates linked to secular variations of weathering processes and reveals the strong denudation and sediment removal conditions of the last glacial stage (15-18 kyr).

The implication of this study is that provenance of Holocene sediments now buried in the floodplain can be determined by a simple comparison with modern sand composition. Sand composition studies may represent a useful tool to reconstruct the Pleistocene-Holocene fluvial sediment supply and the evolution of human settlements as function of climate and drainage system changes.

Keywords: Modena, fluvial sand, provenance, Quaternary

INTRODUCTION

Sand composition studies are useful for reconstructing the sedimentary history of a basin as a function of climatic-physiographic control of sediment production, supply and dispersal (Basu, 1985; Critelli et al., 1997; Weltje et al., 1998). These studies have a particular significance in areas such as the Late Pleistocene-Holocene Modena plain, where fluvial sediments buried a spectacular number of Neolithic, Iron Age, Bronze Age, Etruscan, Roman and Longobardian archaeological sites. The evolution of these human settlements through time can be investigated in detail by reconstructing the palaeogeography of the plain, which has been done mainly by stratigraphic (Gasperi et al., 1989) and geomorphological studies (Cardarelli et al., 2004; Panizza et al., 2004). Palaeochannel traces visible on the surface, for example, may help to reconstruct the ancient local drainage patterns, but the limitation of this method is that only the very late stage evolution of the plain can be investigated. Sediment composition studies may extend our knowledge of the sedimentary supply further back in time through the stratigraphic column, provided that fluvial sediment provenance can be distinguished. Moreover, the good chronological control available for the stratigraphy of the area allow us to investigate in detail the sediment compositional variability through time as a function of late glacial-interglacial climate cycles.

This paper illustrates our studies on the stream sediments in the Modena Plain, where we have compared modern and ancient sands to reconstruct their compositional evolution through time. The purpose of this study is to provide a contribution to the understanding of the fluvial sediment supply to test the possibility to investigate the evolution of human settlements as a function of climate and drainage system changes.

GEOLOGICAL SETTING

The Modena alluvial plain area is located at the northern side of the Northern Apennines thrust- and fold-belt, where streams draining the chain flow toward the north-east into the Po River (Fig. 1). The Northern Apennines formed mainly during the Tertiary as consequence of convergence between the European and the Adria plates. The convergence consumed the interposed Tethyan oceanic crust with the formation of an accretionary prism, which, during the subsequent collisional phase, produced an orogenic wedge consisting of the following tectono-stratigraphic units (Bettelli & De Nardo, 2001):

a) Tuscan-Umbria-Romagna units formed by deformation of the Adria passive margin; in the study area these units consist mainly of Upper Oligocene-Middle Miocene thick siliciclastic turbidite sequences and chaotic shaly assemblages (mélanges);
b) Sub-Ligurian units consisting of Paleocene-Early Miocene siliciclastic and carbonate turbidite sandstones, conglomerates and shales;
c) Ligurian units generated by the subduction of the Tethyan Ocean and represented mainly by Early Cretaceous-Early Tertiary chaotic deep water shaly rocks (mélanges and olistostromes) and calcareous and arenaceous turbidite sandstones; these units contain also Late Jurassic-Early Cretaceous ophiolites, chert and limestones, derived from the former oceanic floor sequence.

The Ligurian thrust-nappe units overlie the Sub-Ligurian thrust-nappe units and both lie on the Tuscan-Umbria-Romagna fold-and-thrust belt units. On the northern side of the chain, the Ligurian units are unconformably overlain by the Epi-Ligurian Sequence and by Miocene-Pliocene and Quaternary terrigenous deposits of the Po Plain. The Epi-Ligurian sequence consists of a thick Middle Eocene-Early Messinian succession of matrix-supported breccias (olistostromes), deep water varicolored shales and marls, muddy and sandstone turbidites, conglomerates, shallow water siliciclastic and bioclastic deposits. The Pliocene deposits consist mainly of marine deep water mudstones.

The Po Plain is the syntectonic sedimentary wedge filling the Pliocene-Pleistocene Apennine foredeep. The total basin infill is up to 4 km thick and the Quaternary deposits reach a thickness of 1.5 km.

CLIMATE AND GEOMORPHOLOGY

The study area has an approximate extent of 150 km^2 and is limited by two major rivers, the Secchia River to the west and Panaro River to the east (see Tab. 1 for river data). The area is crossed by minor streams that mostly drain into the Panaro River (Fig. 2). The drainage basin climate is classified as “temperate subcontinental” (Mennella, 1972). Mean annual temperature varies from 8 to 12° C and coldest and hottest months are January and July, respectively. Precipitation varies with elevation, ranging from 800 to 2400 mm/yr and generally having two maxima during the year, at November and May, and a minimum in July.

As previously described, the streams drain areas that consist mainly of sedimentary rocks, such as arenites, siltstones and shales (Fig. 1). Magmatic rocks crop out along the main valleys as isolated ophiolite blocks including diabase, serpentinite and gabbro suites. No metamorphic rocks are present with the exception of very limited areas at the extreme tip of the Secchia river watershed, where amphibolites and quartzites crop out. River drainage basin data and estimate of the relative proportion of erodable terranes in the catchment areas are reported in Tab. 1 (Cati, 1981). Although the Secchia River has a larger drainage basin than the Panaro River (2174 versus 1784 km^2), the latter includes a larger proportion of erodable terranes and as a result is characterized by a higher suspended load (2030 versus 1847 t/km^2) and an higher inferred soil erosion (0.769 versus 0.684 mm/yr, Tab. 1).
The minor streams drain the northernmost side of the Apennine chain cutting mostly argillaceous and arenite sediments (Fig. 1). Their drainage system in the alluvial plain has been heavily modified since ancient time to limit the impact of floods on urban areas. The Cerca stream (Torrente Fossa), for example, was deviated into the Secchia River in the XV or XVI century (Fig. 2). Gasperi and Pizziolo (in press) report historical accounts that the Tiepido stream was deviated into the Panaro River; unfortunately the year when this deviation took place is unknown.

SAMPLES AND METHODS

A total of 42 samples of modern sands were collected in active longitudinal bars of 9 stream channels (Fig. 2). Sampling covers the channel segments between the point where the stream enters the floodplain and the last downstream occurrence of sand in the stream beds. The sampling network was designed to obtain sand specimens at approximately the same spacing distance for the each stream and to include, where possible, upstream and downstream confluence points.
A total of 9 ancient sands were collected from river cuts, archaeological sites and cores located in the channel belt of the main rivers (Fig. 2). Unfortunately no sections with archaeological remains and ancient sand sediments are available for the minor streams. Hereafter ancient sediments younger than the Late Pleistocene are called “Holocene” sands, whereas the term “modern” is restricted to present-day settings.
Sand samples were washed with dilute H_2O_2 to remove organic matter, air dried and sieved to obtain the fine sand fraction (0.125-0.250 mm, 3-2 ϕ). The necessity to analyze the fine sand fraction was dictated by the lack of medium-coarse sand at some of the sampling sites. The fine sand fraction was impregnated in epoxy resin under vacuum, thin-sectioned and stained for feldspar and carbonate identification.
Point-counting under transmitted light microscopy was performed according to the Gazzi-Dickinson method (Gazzi, 1966; Dickinson, 1970; Zuffa, 1985; Ingersoll et al, 1984). At least 300 grains were point-counted for each section to achieve modal composition and 40 categories of grains were distinguished. Results of point-counting are illustrated in Tab. 2. Components not related to the original sand composition, such as brick and pottery fragments, penecontemporaneous shell fragments and authigenic carbonate nodules, were excluded from the final calculations.
Statistically rigorous confidence regions of the studied samples were calculated according to Weltje (2002). Error bars in the diagrams were calculated according to Howarth (1998).

RESULTS

Modern sands

The modal analyses show that modern stream sands in the Modena plain have a similar overall compositions, but show significant variations in quartz, feldspar, carbonate and lithic fragment contents (Tab. 2, Fig. 3, Fig. 4). Plotting the data in Q+F–Total carbonates–Lithic fragments ternary diagram, the compositional fields reveal that sediments from different modern streams can be clearly distinguished (Fig. 4).
Streams draining the eastern sector of the study area (Panaro, Tiepido, Guerro) have a generally higher carbonate content than those draining the western part, which are enriched in quartz and feldspar (Secchia and Grizzaga).
The most distinctive compositions are those of Guerro and Tiepido, which have the highest carbonate content, mainly represented by single calcite crystals (Fig. 4; Tab. 2).
The Grizzaga stream shows the greatest variation in terms of the measured parameters, and therefore has the broadest compositional field (Fig. 4).

Holocene sands (< ~7 kyr)

Ancient sands collected in the channel belt of the major rivers (ages given by Gasperi and Pizziolo, in press) provide an exceptional and unique view of the compositional variations of the sediment through time. The Panaro River deposits at Spilamberto (Fig. 2) buried a spectacular series of Neolithic, Roman and Longobardian sites, and we can observe a complete sedimentary section ranging in age from the Late Pleistocene to present day (Fig. 5). The samples younger than ~7 kyr plot very close to the compositional field of modern sands (Fig. 6). In particular, these sands are slightly enriched in carbonate and lithic fragments and impoverished in quartz, compared with the modern ones (Fig. 6; Tab. 2).
We analyzed two Holocene sands from the Secchia River: one has an inferred age of between 3540 ± 50 and 4585 ± 95 B.P. (sample FS B) and the other is slightly older than 4585 ± 95 B.P. (sample FS C; Tab. 2; correlation with data from Cremaschi, 2000). These two samples plot directly into the compositional field of the modern sands (Fig. 6).

Late Pleistocene sands (> 10-12 kyr)

Ancient sands from fluvial deposits that are attributed to the last glacial event (Vignola Unit, Late Pleistocene, age 15-18 kyr, Gasperi and Pizziolo, in press) have higher contents of quartz and feldspar compared to both modern and Holocene sands (Tab. 2). The feldspar content in Late Pleistocene sands (age >12 kyr) from cores located a few km north of Modena range from 13.5 to 30.8% (Lugli et al., 2004), whereas the range in the modern sands is from 6.9 to 21.3% (Tab. 2).
Higher feldspar abundances have also been detected in the Late Pleistocene sands from the Panaro River channel belt at Spilamberto (Fig. 2). Here, as shown in Fig. 7, feldspar content is highest in the Late Pleistocene (14.9-18.4%, Tab. 2), decreases in the Holocene (10.5-13.1%) and remains constant in the modern sediments (10.3-15.3%) with the noticeable exception of sample P12 (18.1%; Tab. 2) which, as discussed later, is influenced by direct supply of eroded Pleistocene sediments.

SEDIMENT DIAGENESIS

Correct interpretation of compositional data requires an understanding of the diagenetic processes that may have affected ancient sands. In the Modena plain, post-depositional modifications that may have altered the provenance signal of the sands are: chemical weathering of feldspar grains to form clay minerals and Al-hydroxides, dissolution of carbonate clasts and growth of carbonate concretions.

Survival of feldspar in the rock record is strongly influenced by climatic conditions during sediment production, storage and dispersal (James et al., 1981; McBride et al., 1996; Critelli et al., 2003). Feldspar preservation during burial diagenesis may be roughly evaluated by the relative proportions of altered versus unaltered grains. Point-counting of feldspar populations in the modern sands indicates that content of altered and unaltered feldspar grains is approximately the same (49-66%). The proportion does not vary downstream in modern sands and remains approximately the same in the Holocene buried sediments (Panaro River). On the other hand, the most ancient sands that we analyzed (Late Pleistocene, age 15-18 kyr) have more abundant feldspar than the modern and Holocene sands (age <~7 kyr; Lugli et al., 2004) suggesting that post depositional chemical weathering during burial has not caused any significant selective destruction of feldspar grains (Fig. 3e).
Carbonate sand grains can be dissolved by groundwater, but our observations suggest that dissolution phenomena have not significantly changed the composition of the analyzed sediments. Observations under the microscope show that most calcite clasts (single calcite crystals) are not corroded and show distinctive rhombohedral angular shapes (Fig. 3b and c), a feature that is incompatible with post-depositional dissolution. Removal of carbonate components also appears to have been negligible because buried ancient sands have generally higher carbonate content than the modern ones (Panaro River, Fig. 6). Limited partial dissolution preferentially affected microcrystalline carbonate grains, but total dissolution leading to grain removal was probably mainly concentrated in the very fine grained fractions (<0.125 mm), and thus did not obliterate the original composition revealed by point-counting of the 0.125-0.250 mm size fraction.
Caliche formation is the main diagenetic process in the ancient sediments and affects also relatively young sediments that buried Roman Age artefacts (I-II AD). These microcrystalline carbonate nodules range in size from fractions of mm to a few cm and are usually concentrated in thin layers. The caliches have grown displacively into the fine-grained sediments (clay and silt) and are commonly associated with roots (Fig. 3f). Very small nodules, up to a few fractions of mm in size, may be present also in the sand layers. Their formation is early and linked to groundwater table oscillations and to the development of soils (Maffei, 2001). As discussed earlier, their presence in the ancient sand does not compromise the definition of the original composition because they can be easily recognized under the microscope as secondary particles and excluded from the calculations. In particular cases, such as recycling of older sediments, some of the eroded caliche fragments may be difficult to distinguish from microcrystalline carbonate grains. As a consequence, point-counting could overestimate the microcrystalline carbonate content of some modern sand, but, as discussed earlier, the carbonate content is slightly higher in Holocene than in modern sands (Panaro River, Tab. 2; Fig. 6).

DOWNSTREAM COMPOSITIONAL VARIATIONS: RECYCLING AND MIXING

The broad field composition of modern sand is due to both mixing of different sands at confluence points and recycling of older sediments along stream. Ancient sand deposits are cut and eroded by the main rivers (between sampling sites P 12 and P A for the Panaro River and between FS A and FS 9 for the Secchia River, Fig. 2). Because the compositions of the Holocene sands are similar to those of the modern sands, mixing of similar end members would not cause significant deviation of sediment composition downstream.
The only difference could be an increase of shale grains due to erosion of fine-grained sediments associated with the Holocene sands (Fig. 5). By contrast, Late Pleistocene sands are not usually associated with fine-grained sediments and differ considerably in composition. For this reason, recycling of Late Pleistocene sands produces a large compositional variation in modern sands.

The complex downstream compositional variations for the Secchia and Panaro Rivers are illustrated in Figs 8 and 9, respectively.
The Secchia River compositional diagram can be divided in two parts: upstream and downstream of sampling site FS A (Fig. 8). In the upstream part the compositional pattern is characterized by a decrease in feldspar and lithic fragments and an increase in quartz content. This represents the expected trend by downstream labile grain destruction during transport. An exception is represented by the content of single calcite crystals, which increase downstream. This suggests that the main grain degradation mechanism is probably not abrasion, but mechanical breakage along cleavage planes. This process produces new smaller calcite rhombohedra, multiplying their content in the fine sand fraction. This hypothesis is supported by the observation that most single calcite grains show distinct rhombohedral shapes (Fig. 3a and d) in all sand fractions and that microcrystalline carbonate rock fragments decrease downstream, rather than increase. Mixing of sand input from the tributaries does not appreciably influence the composition of the Secchia River sediments, with the exception of the Fossa stream. The Fossa sand has a higher content of micritic carbonate grains, causing a reversal in the general decreasing trend shown by this grain type just after the confluence (between sampling sites FS 11 and FS 2, Fig. 8).

The downstream part of the Secchia River diagram shows a marked feldspar increase. This behaviour is related to new detrital input resulting from erosion of Late Pleistocene sediments, which have higher feldspar contents than modern and Holocene sands. This recycled sediment input, as we have verified in the field, is restricted to between sampling sites FS A and FS 7; at sample site FS 9 further downstream, the expected pattern of labile grain decrease (Fig. 8) returns.
In the Panaro River, downstream compositional variations are more complex. Most labile grains such as shale, siltstone and micritic carbonate fragments show such dramatic fluctuations that they cannot be simply related to mixing of different sands derived from the tributaries (Fig. 9). In this case, erosion of Holocene fine-grained river sediments results in multiple inputs of labile fragments that produce concurrent dilution effects exceeding by far the variations that related to the tributary streams. The marked increase in feldspar content at sampling site P 12 is the result of recycling of feldspar-rich Late Pleistocene sediments that are directly eroded in the riverbed. The feldspar signal is then attenuated after a few km possibly by grain abrasion/breakage, but most probably by downstream dilution, as testified by increase of other labile grains such as shale and siltstone fragments derived through erosion of Holocene river sediments (Fig. 9).
Ophiolite fragments, which are by far the less abundant of the lithic fragments, appear to behave conservatively in both the Panaro and Secchia Rivers (Figs 8 and 9). Their content does not significantly change downstream in all studied streams and appears to be transport invariant, as discussed by Weltje and Von Eynatten, (2004).
The complex downstream compositional variations of the sands are shown schematically in Fig. 10. Although the interpretations proposed in this study should be confirmed by further analyses, it is important to note that the number of samples examined from this relatively small system is high compared with most similar studies reported in the literature

DISCUSSION

Modern sands composition: extent of watershed and recycling

On the basis of the available data, the compositional fields of the modern stream sands appear to be linked to: a) the extent of the watershed, b) recycling of ancient fluvial sediments, and c) sediment input from tributary streams.

The extent of the watershed appears to be the dominant factor controlling sand composition. This effect is directly related to the setting of bedrock units that are mostly oriented parallel to the Apennine margin and normal to the drainage systems (Fig. 1). The most distinctive sand compositions are those of the streams characterized by smaller watershed where sediment supply is deriving from only one or a few geological formations. This is the case of the Guerro and Tiepido streams, which display the most extreme sand compositions, exemplified by their high carbonate content (Fig. 4).
Recycling of ancient sediments, in particular the Late Pleistocene sands, which are particularly rich in feldspar, is the main factor that causes widening of the modern sediment composition fields. This effect is particularly evident for the Panaro River, which also receives a significant input of labile grains by erosion of ancient sediments (Fig. 9).
Sediment input from tributaries has a subordinate effect on sediment composition because minor streams generally provide sand that is not dramatically different in composition. However, the Nizzola stream that is a tributary of the Panaro River (Tab. 2; Fig. 2) represent an exception to this rule: sands differ significantly, being the Nizzola sand higher in quartz and lower in carbonates, but sediment input at confluence is very scarce and does not influence the Panaro River sand composition.

Holocene sands: a constant composition

Our data demonstrate that sand composition of the main rivers has not varied significantly in the last 7 kyr. Although constant sand composition for this time span can be demonstrated only for the major rivers (Panaro and Secchia), it seems reasonable that sediment composition of minor streams would also not have varied. On the other hand, palaeochannel traces and historical records indicate that the minor streams changed flow patterns many times, both by natural avulsions and artificial diversions (Gasperi and Pizziolo, in press). The result is that minor stream sediment supply patterns changed markedly through time, as a consequence of different confluence networks and different contributions of recycled older sand in their pathway. Thus, ancient sand compositions of minor streams are probably different to the modern streams. We are currently investigating this hypothesis by sampling palaeochannel sediments.

Late Pleistocene sand composition: the glacial signal

The significant shift in sand composition for sediments older than ~12 kyr, with an overall higher content of quartz and feldspar components could be explained by various factors: a) tectonics, b) diagenesis and c) climatic effects.
A change in the bedrock lithology induced by neotectonics could modify the sediment supply to the basin. Tectonics and climate are considered to be the major controlling factors for the Quaternary alluvial architecture at the southern margin of the Po basin in the Bologna area (Fig. 1; Amorosi et al., 1996). On the other hand, the latest documented tectonic uplift of the chain ended in the Reggio Emilia sector in the Late Pleistocene and the continental Late Quaternary deposits onlapping the Apennine margin appear undeformed (Barbacini et al., 2002).
Moreover, as discussed earlier, post-depositional diagenetic changes, such as feldspar alteration and carbonate dissolution, do not seem to have varied the sand composition.
Climate changes related to glacial-interglacial phases appear to be the most important factor that modified sediment composition at ~12 kyr by changing bedrock weathering rate and removal of weathering products. This shift in composition represents a clear supply signal in the basin fill record. High-frequency variations in the rate of sediment supply (order of 10 kyr) are recorded as secular variations of the extent of weathering (Weltje et al., 1998). The

change in composition suggests that sediments are today subjected to more prolonged chemical weathering during storage in the source area, but that alteration was negligible during storage in the alluvial sequence, at the contrary of what is reported for tropical climate settings (Johnsson et al., 1991). Thus, the sediment supply shift could reflect changes from a stage of marked denudation, such as during the last glacial maximum (15-18 kyr, Orombelli and Ravazzi, 1996) to a stage of colluvial aggradation and soil formation with dense vegetation cover (since ~7 kyr).

CONCLUSIONS

In the Late Pleistocene-Holocene sedimentary record of the Modena floodplain, the composition of fluvial sands has provided an unique opportunity to recognize and isolate the signature of factors controlling sediment supply and the nature of their complex interactions.
Modal analyses of modern sands from the Modena Plain streams indicate that their provenance signal can be clearly distinguished. The compositional field of modern sands from each stream depends, in order of importance, on the extent of the watershed, the recycling of older fluvial sediments and, subordinately, on the sediment input from tributary streams.
Our data demonstrate that sand composition of major rivers (Panaro and Secchia) has not varied since the last ~7 kyr, a stage characterized by colluvial aggradation with dense vegetation cover. The direct implication is that provenance of older sediments buried in the floodplain can be determined by a simple comparison with modern sand composition, suggesting that we have a powerful tool to reconstruct the evolution of the main drainage system in the Holocene. The next step will be to extend this study to characterize the evolution of human settlements as a function of drainage system changes.
The higher feldspar content in Late Pleistocene fluvial sands appears to reflect a high-frequency signal in sediment supply rate due to secular variations of weathering processes. This compositional shift reveals the strong denudation and sediment removal conditions of the last glacial stage (15-18 kyr). For these reasons, sand composition studies represent a new, fundamental key to investigate the glacial-interglacial climatic influence on sediment supply and deposition in the northern Apennines floodplain.

ACKNOWLEDGEMENTS

We thank N. Giordani (Soprintendenza per i Beni Archeologici dell’Emilia Romagna) for permission to sample archaeological sections. We are grateful to D. Vai and A. Ferrari for support in archaeological sites. The thoroughly and constructive reviews of A.C. Morton, M. Johnsson and G.G. Zuffa greatly improved the manuscript.

REFERENCES CITED

Amorosi, A., Farina, M., Severi, P., Preti, D., Caporale, L., and Di Dio, G., 1996, Genetically related alluvial deposits across active fault zones: an example of alluvial fan-terrace correlation from the upper Quaternary of the southern Po Basin, Italy: Sedimentary Geology, v. 102, p. 275-295.

Barbacini, G., Bernini, M., Papani, and G., Rogledi, S., 2002, Le strutture embricate del margine appenninico emiliano tra il T. Enza ed il F. Secchia- Prov. Reggio Emilia: Cartografia Geologica, Atti III seminario sulla cartografia geologica, Bologna, 26-27 febbraio 2002, p.64-69.

Basu, A., 1985, Influence of climate and relief on compositions of sands released at source areas: G.G. Zuffa, Editor, Provenance of Arenites, NATO ASI series, D. Reidel Publishing Company, v. 148, p. 1–18.

Bettelli, G., and De Nardo, M.T., 2001, Geological outlines of Emilia Apennines (Italy) and introduction to the rock units cropping out in the areas of landslides reactivated in the 1994-1999 period: Quaderni di Geologia Applicata, v. 8(1), p. 7-26.

Cardarelli, A., Cattani, M., Labate, D., and Pellegrini, S., 2004, Archeologia e Geomorfologia. Un approccio integrato applicato al territorio di Modena: Per un Atlante Storico Ambientale Urbano, Comune di Modena, Ufficio Ricerche e Documentazione sulla Storia Urbana, p. 65-77.

Cati, L., 1981, Idrografia e idrologia del Po: Ufficio Idrografico del Po, Istituto Poligrafico e Zecca dello Stato, Pubblicazione 19, 310 p.

Cremaschi, M., 2000, Manuale di geoarcheologia, Editori Laterza, 386 p.

Cremaschi, M., and Gasperi, G., 1989, L'alluvione alto medioevale di Mutina (Modena) in rapporto alle variazioni ambientali oloceniche: Memorie delle Società Geologica Italiana, v. 42, p.179-190.

Critelli, S., Arribas, J., Le Pera, E., Tortosa, A., Marmaglia, K.M., and Latter, K.K., 2003, The recycled orogenic sand provenance from an uplifted thrust belt, Betic Cordillera, southern Spain: Journal of Sedimentary Research v. 73 (, p. 72–81.

Critelli, S., Le Pera, E., and Ingersoll, R.V., 1997, The effects of source lithology, transport, deposition and sampling scale on the composition of southern California sand: Sedimentology, v. 44, p. 653–671

Dickinson, W.R., 1970, Interpreting detrital modes of graywacke and arkose: Journal of Sedimentary Petrology, v. 40, p. 695-707.

Gasperi, G., and Pizziolo, M., in press, Note illustrative della Carta Geologica d'Italia a scala 1:50.000. Foglio 201 "Modena": Regione Emilia-Romagna, Servizio Geologico d'Italia.

Gasperi, G., Cremaschi, M., Mantovani Uguzzoni, M.P., Cardarelli, A., Cattani, M., and Labate, D., 1989, Evoluzione plio-quaternaria del margine appenninico modenese e dell'antistante pianura. Note illustrative alla carta geologica: Memorie delle Società Geologica Italiana , v. 39, p. 375-431.

Gazzi, P., 1966, Le arenarie del flysh sopracretaceo dell'Appennino modenese; correlazioni con il Flysh di Monghidoro: Acta Mineralogico-Petrographica, v. 12, p. 69-97.

Howarth, R.D., 1998, Improved estimators of uncertainty in proportions, point-counting, and pass–fail text results: American Journal of Science, v. 298, p. 594–607.

Ingersoll, R.V., Bullard, T.F., Ford, R.L., Grimm, J.P., Pickle, J.D. and Sares, S.W., 1984, The effect of grain size on detrital modes: a test of the Gazzi–Dickinson point-counting method: Journal of Sedimentary Petrology, v. 54, p. 103–116.

James, W.C., Mack, G.H., and Suttner, L.J., 1981, Relative alteration of microcline and sodic plagioclase in semi-arid and humid climates: Journal of Sedimentary Petrology, v. 51, p. 151-163.

Johnsson, M.J., Stallard, R.F., and Lundberg, N., 1991, Controls on the composition of fluvial sands from a tropical weathering environment; sands of the Orinoco River drainage basin, Venezuela and Colombia: Geological Society of America Bulettin, v. 103, p. 1622–1647.

Lugli, S., Marchetti Dori, S., Fontana, D., and Panini, F., 2004, Composizione dei sedimenti sabbiosi nelle perforazioni lungo il tracciato ferroviario ad Alta Velocità: indicazioni preliminary sull'evoluzione sedimentaria della media pianura modenese: Il Quaternario, v. 17, p. 379-390.

Maffei, M., 2001, Evoluzione recente della pianura modenese-reggiana, implicazioni paleoambientali, paleoclimatiche e geoarcheologiche: unpublished doctorate thesis, University of Modena e Reggio Emilia.

McBride, E.F., Abel-Wahab, A., and McGilvery, T.A., 1996, Loss of sand-size feldspar and rock fragments along the South Texas Barrier Island, USA: Sedimentary Geology, v. 107, p. 37-44.

Mennella, C., 1972, Il clima d'Italia: volume secondo, Fratelli Conte Editore, Napoli, Italy, 803 p.

Orombelli, G., and Ravazzi, C., 1996, The Late Glacial and Early Holocene chronology and paleoclimate: Il Quaternario, v. 9, p. 439-444.

Panizza, M., Castaldini, D., Pellegrini, M., Giusti, C., and Piacentini, D., 2004, Matrici geo-ambientali e sviluppo insediativo: un'ipotesi di ricerca: Per un Atlante Storico Ambientale Urbano, Comune di Modena, Ufficio Ricerche e Documentazione sulla Storia Urbana, p. 31-62.

Weltje, G.J., 2002, Quantitative analysis of detrital modes: statistically rigorous confidence regions in ternary diagrams and their use in sedimentary petrology: Earth-Science Reviews., v. 57, p. 211–253.

Weltje, G.J., and Von Eynatten, H., 2004, Quantitative provenance analysis of sediments: review and outlook: Sedimentary Geology, v. 171, p. 1-11.

Weltje, G.J., Meijer, X.D., and De Boer, P.L, 1998, Stratigraphic inversion of siliciclastic basin fills: a note on the distinction between supply signals resulting from tectonic and climatic forcing: Basin Research, v. 10, p. 129–153.

Zuffa, G.G., 1985, Optical analyses of arenites: influence of methodology on compositional results: G.G. Zuffa, Editor, Provenance of Arenites, NATO ASI series, D. Reidel Publishing Company, v. 148, p. 165-189.

FIGURE CAPTIONS

Fig. 1 - Geological sketch of the drainage basins of the Secchia and Panaro River in the northern Apennines. Simplified from Bettelli and De Nardo (2001).

Fig. 2 - Simplified sketch of the fluvial drainage network in the Modena Plain with sampling sites of modern and ancient sands.

Tab. 1 - Physiographic characteristics of Secchia and Panaro River drainage basins.

Fig. 3 – Photomicrograph of diagnostic grains in fluvial sands from the Modena Plain. A) Modern sand from the Panaro River (sample P 9). Most single calcite grains (c) show distinct rhombohedral shape.
B) Holocene sand from the Panaro River (sample S 2); A large rhombohedral calcite grain is visible (c).
C) Late Pleistocene sand from the Panaro River (sample S 10); notice the rhombohedral calcite grains (c).
D) Modern sand from the Secchia River (sample FS 6); Rhombohedral calcite grains (c) are common.
E) Altered plagioclase (p) and unaltered feldspar grains in Late Pleistocene Panaro River sand (sample S 8).
F) Carbonate concretions (caliche) (sample from Modena urban area); notice the hollow concretion at center that probably developed around a root; a shell fragment from a thin-walled gastropod (Bp) is also visible.
All photograph are in cross polarized light. C, calcite single crystal; Ca, caliche; Bp, bioclast (penecontemporaneous); Bt, bioclast (terrigenous); Cm, carbonate mudstone; K, potassium feldspar; M, microcline; P, plagioclase; Q, quartz (monocrystalline); Qp, quartz (polycrystalline); S, siltstone; Sl, silty-limestone; Sh, shale.

Tab. 2 – Results of petrographic modal analyses.

Fig. 4 – Ternary diagrams showing modern sand composition of the Modena Plain streams. Additional ternary diagram (right) show 90% confidence regions of the mean for each stream sand (according to Weltje, 2002).

Fig. 5 - Simplified stratigraphic sketch of the Spilamberto quarry. Late Pleistocene braided channel gravels are overlain by Holocene overbank fines. The latter are in turn cut by a recent channel and by the present-day riverbed. Sampled sands are shown by black arrows. White arrows indicate archaeological layers. Vertical arrows show the general altimetry, not to scale.

Fig. 6 - Ternary diagrams showing the composition of Holocene sand from the Modena Plain major rivers (Secchia and Panaro). Compositional fields of modern stream sands are also reported.

Fig. 7 - Plot of feldspar content in sands from the Spilamberto quarry as function of archaeological chronology. Samples younger than Longobardian Age are plotted in an arbitrary vertical scale to show their relative age; true stratigraphic relationships are shown in Fig. 5. Error bars calculated according to Howarth (1998).

Fig. 8 – Plot of downstream compositional variability of Secchia River sands as a function of distance from source and confluence points of tributary streams (arrows). a) recalculated parameters, b) all grain types. Errors bars are not reported for simplicity; error bar amplitudes

are similar to those reported in Fig. 9. Sites with more than one sample are reported as mean of measured parameters.

Fig. 9 - Plot of downstream compositional variability of Panaro River sands as a function of distance from source and confluence points of tributary streams (arrows). a) recalculated parameters, b) all diagnostic grain types. Sites with more than one sample are reported as mean of measured parameters. Error bars calculated according to Howarth (1998).

Fig. 10 – Sketch summarizing the downstream compositional variations of the modern stream sands as a function of transport and erosion of ancient sediments.

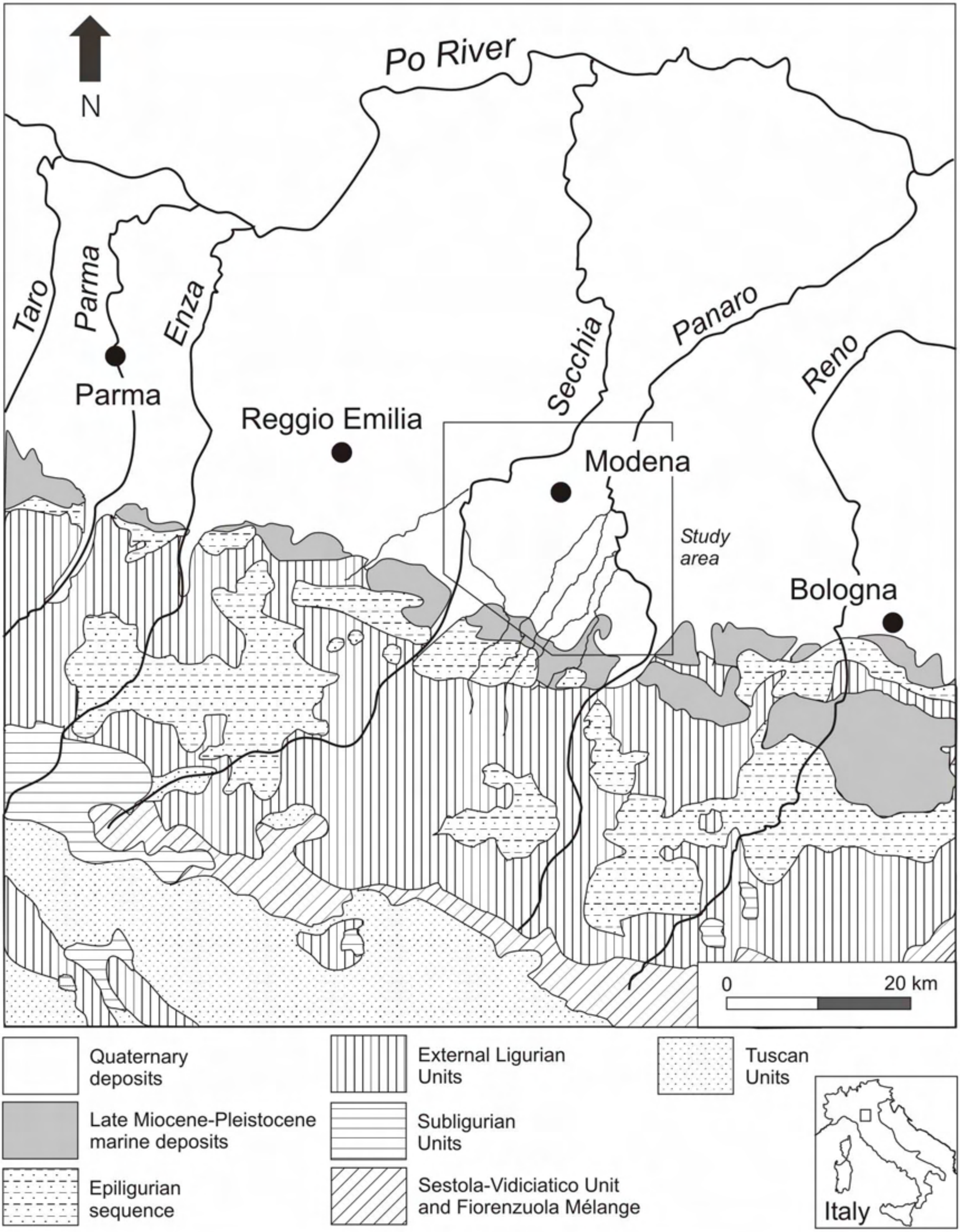
N
Po River
Taro
Parma
Enza
Secchia
Panaro
Reno
Parma
Reggio Emilia
Modena
Bologna
Study area
0
20 km
Quaternary deposits
Late Miocene-Pleistocene marine deposits
Epiligurian sequence
External Ligurian Units
Subligurian Units
Sestola-Vidiciatico Unit and Fiorenzuola Mélange
Tuscan Units
Italy

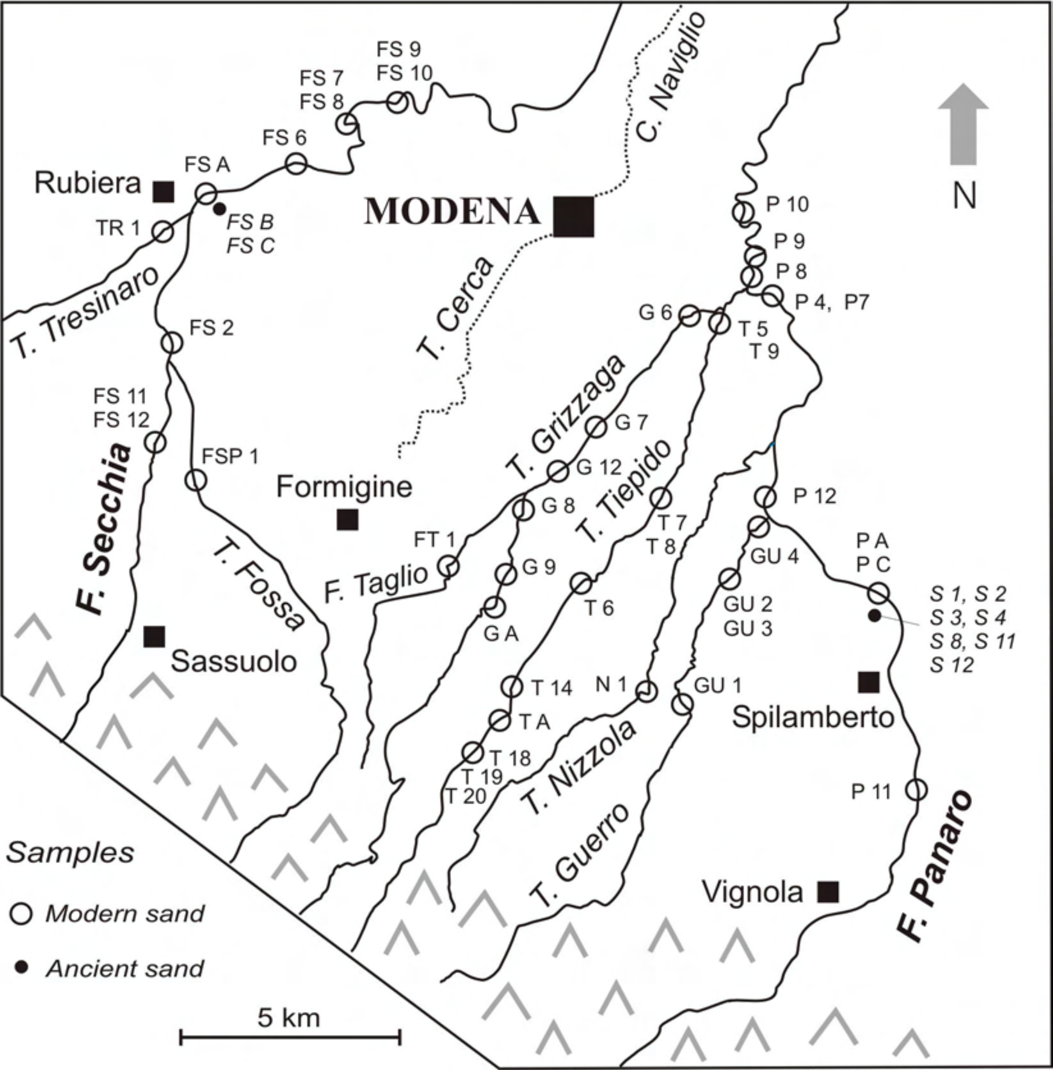

FS 9
FS 10
FS 7
FS 8
C. Naviglio
FS 6
FS A
Rubiera
MODENA
N
TR 1
FS B
FS C
P 10
P 9
P 8
P 4, P7
T. Tresinaro
T. Cerca
G 6
T 5
T 9
FS 2
T. Grizzaga
FS 11
FS 12
G 7
F. Secchia
FSP 1
G 12
T. Tiepido
Formigine
G 8
P 12
T 7
T 8
FT 1
T. Fossa
G 9
GU 4
P A
P C
F. Taglio
T 6
G A
GU 2
GU 3
S 1, S 2
S 3, S 4
S 8, S 11
S 12
Sassuolo
T 14
N 1
GU 1
Spilamberto
T A
T. Nizzola
T 18
T 19
T 20
P 11
F. Panaro
T. Guerro
Samples
Modern sand
Ancient sand
Vignola
5 km

	Secchia River	Panaro River
Drainage basin		
Area (km^2)	2174	1784
Maximum (m.s.l.)	2121	2165
Minimum (m.s.l.)	14	10
Range (m.s.l.)	2107	2155
Mean (m.s.l.)	606	662
Highly erodible terranes (%)	30,7	45,3
Medium erodible terranes (%)	25,8	15
Low erodible terranes (%)	43,5	39,7
River channel		
Length (km)	170	160
Average discharge (m^3/s)	27,2	23,7
Suspended load (t/km^2)	1847	2030
Inferred soil erosion (mm/yr)	0,684	0,769

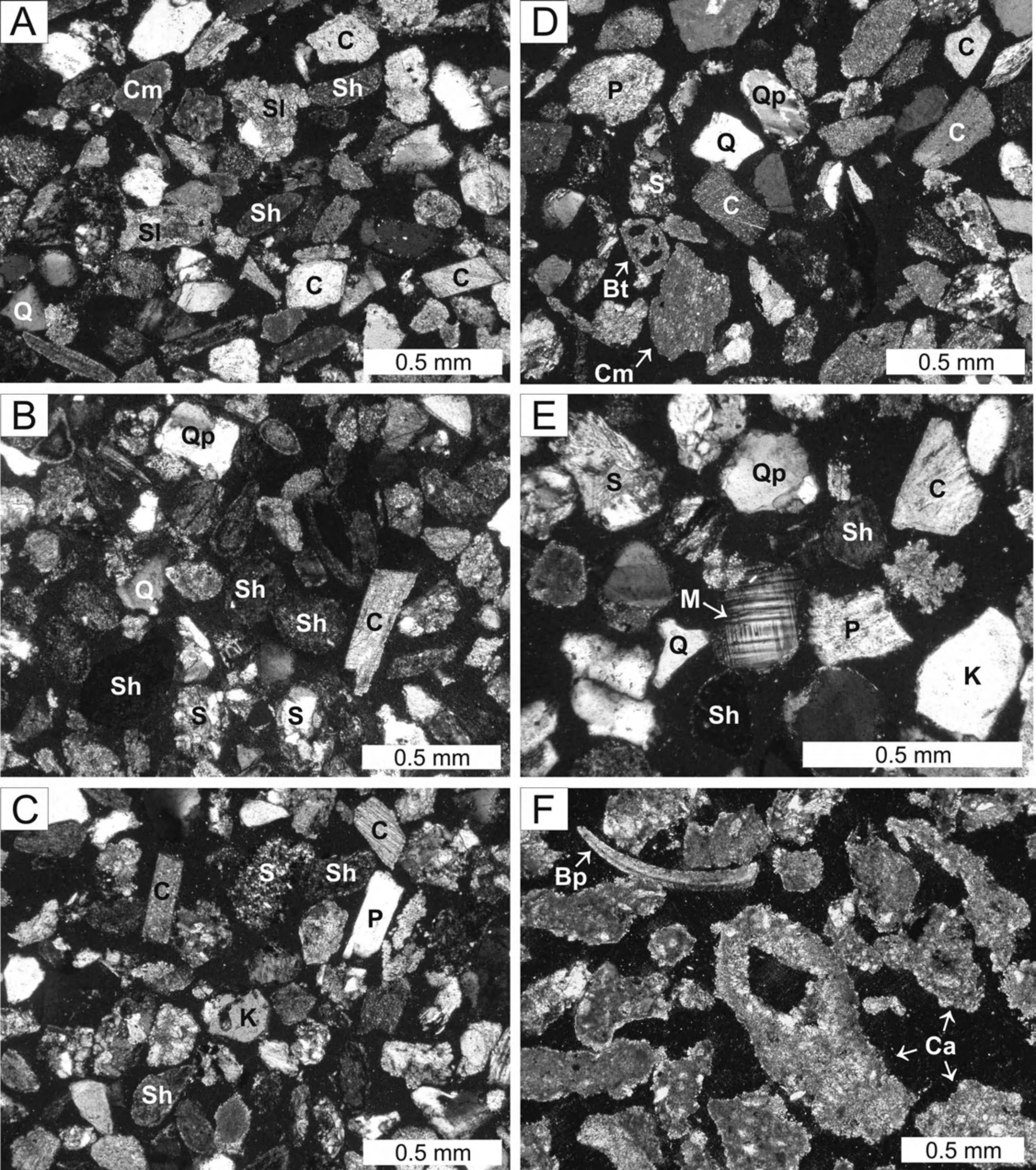

A
C
Cm
Sh
Sl
Sh
Sl
C
C
Q
0.5 mm
D
C
P
Qp
Q
C
S
C
Bt
Cm
0.5 mm
B
Qp
Q
Sh
Sh
C
Sh
S
S
0.5 mm
E
S
Qp
C
Sh
M
Q
P
K
Sh
0.5 mm
C
C
S
Sh
C
P
K
Sh
0.5 mm
F
Bp
Ca
0.5 mm

			Tresinaro	Secchia											Fossa	Taglio	Grizzaga						Tiepido					
			Modern	*Modern*									*Holocene*		*Modern*	*Modern*	*Modern*						*Modern*					
		Sample	TR 1	FS 11	FS 12	FS 2	FS A	FS 6	FS 7	FS 8	FS 9	FS 10	FS B	FS C	FSP 1	FT 1	G A	G 9	G 8	G 12	G 7	G 6	T 18	T 19	T 20	T A	T 14	T 6
NCE	Q	Quartz single crystal	11,8	9,6	11,2	18,9	15,2	17,7	13,5	21,2	19,2	20,2	13,1	17,0	12,4	14,4	22,3	20,8	9,8	19,5	15,2	20,8	7,7	10,6	10,4	11,6	11,3	10,3
		Quartz polycrystalline coarse texture	2,2	3,9	2,1	1,6	3,8	4,0	2,7	1,9	2,7	3,4	2,2	1,6	2,1	1,6	4,1	1,7	0,9	2,9	3,6	3,9	1,7	1,4	1,7	1,2	1,5	3,1
		Quartz polycrystalline fine texture	3,7	1,5	0,6	1,6	1,9	3,7	1,2	1,9	2,7	2,8	1,2	2,2	1,5	1,6	1,4	1,7	1,2	1,1	1,5	1,8	2,0	0,9	1,7	1,5	0,9	1,2
		Chert	0,9	0,9	0,9	0,9	0,6	-	-	0,6	0,9	0,6	0,3	0,9	0,3	1,0	1,2	2,0	0,6	1,1	0,9	0,3	0,6	1,4	1,7	-	1,7	0,9
		Quartz in plutonic-gneissic rock fragment	1,9	2,7	3,0	0,3	3,5	0,9	1,5	0,3	2,1	2,1	0,9	1,3	1,2	-	2,9	1,1	0,9	0,9	0,6	0,9	-	-	0,3	0,6	0,6	0,3
		Quartz in metamorphic rock fragment	0,3	-	-	0,6	0,9	0,3	0,3	-	0,3	0,3	-	0,3	-	-	-	0,6	-	0,9	-	-	-	-	-	-	0,6	0,3
		Quartz in volcanic rock fragment	-	-	-	-	-	-	-	-	-	-	-	-	-	-	-	-	-	-	-	-	-	-	-	-	-	-
		Quartz in clastic rock fragment	0,3	1,2	0,9	1,9	0,9	1,8	2,4	0,3	0,9	0,9	0,9	1,6	1,8	1,6	1,4	2,5	2,4	1,4	1,2	0,3	3,7	2,3	1,4	1,5	2,6	0,9
	K	K-feldspar single crystal	9,0	6,3	5,2	6,3	3,2	8,0	10,8	9,7	5,8	7,4	4,7	3,1	4,2	2,6	6,4	13,5	8,6	7,2	7,3	8,4	4,3	2,6	3,2	3,3	3,2	3,1
		K-feldspar in plutonic-gneissic rock fragment	0,9	0,9	1,2	0,3	0,9	1,2	1,2	3,1	0,3	0,9		0,9	0,6		0,6	1,4	0,9	0,3	0,3	0,9	0,6	-	0,6	0,3	-	
		K-feldspar in metamorphic rock fragment	-	-	-	-	-	-	-	-	-	-	-	-	-	-	-	0,3	-	-	-	-	-	-	-	-	-	-
		K-feldspar in volcanic rock fragment	-	-	-	-	-	-	-	-	-	-	-	-	-	-	-	-	-	-	-	-	-	-	-	-	-	-
		K-feldspar in clastic rock fragment	-	-	-	-	-	0,3	0,3	-	0,6	0,6	-	-	0,3	-	0,3	-	-	0,3	-	-	-	0,6	0,3	0,3	-	-
	P	Plagioclase single crystal	6,8	5,4	13,4	7,5	6,3	7,0	8,4	5,3	10,1	6,7	11,2	11,0	4,5	4,8	8,1	7,0	5,9	6,9	9,4	6,3	4,0	3,4	2,6	2,7	2,9	6,2
		Plagioclase in plutonic-gneissic rock fragment	-	2,4	0,9	0,3	0,3	0,6	2,4		0,3	0,3	0,9	0,9	0,3	1,3	0,9	0,3	0,6	1,1	0,6	1,5	1,4	1,1	0,3	-	0,6	0,3
		Plagioclase in metamorphic rock fragment	-	-	-	-	-	-	-	-	-	-	-	-	-	-	-	-	-	-	-	-	-	-	-	-	-	-
		Plagioclase in volcanic rock fragment	-	-	-	-	-	-	-	-	-	-	-	-	-	-	-	-	-	-	-	-	-	-	-	-	-	-
		Plagioclase in clastic rock fragment	-	0,9	0,3		0,3		0,3	0,3	0,3	-	-	-	-	0,3	0,6	0,3	1,2	0,6	0,3	-	-	0,9	0,6	0,3	0,6	-
	L	Metamorphic rock fragment	-	-	-	0,3	0,6	1,2	0,3	0,6	1,2	1,5	-	0,3	-	-	0,6	-	-	-	-	-	-	-	-	-	-	-
		Volcanic rock fragment	-	-	-	-	-	-	-	-	-	-	-	-	-	0,3	-	-	-	-	-	-	-	-	-	-	-	-
		Hypoabyssal lithic	-	-	-	-	1,9	-	-	-	-	-	-	-	-	-	-	-	-	-	-	-	-	-	-	-	-	-
		Spilite	0,3	1,5	1,5	0,6	0,3	0,9	1,5	1,9	1,8	3,4	-	0,6	0,6	-	-	-	0,6	0,3	-	-	-	-	-	-	0,3	-
		Serpentinite	5,6	2,4	2,1	2,2	2,5	3,4	1,5	2,8	1,5	1,8	1,9	1,6	1,5	1,9	0,6	0,6	0,9	1,4	0,6	0,6	0,6	0,3	-	0,3	0,3	0,6
		Clastic lithic Shale	9,0	18,3	14,3	14,2	12,0	11,0	9,6	9,7	8,2	10,4	16,2	16,0	9,1	10,6	5,2	4,5	11,2	6,0	6,4	3,6	12,2	12,9	11,5	11,9	11,9	10,6
		Siltstone	10,2	11,4	10,6	9,7	10,8	7,3	8,7	8,7	8,5	8,3	11,8	9,1	9,4	9,3	8,4	4,8	8,9	5,7	8,8	4,8	9,7	9,2	7,5	7,0	9,9	9,7
	M	Muscovite+Chlorite single crystal	0,6	0,6	-	0,6	-	-	-	0,3	0,3	-	1,2	0,6	-	0,3	0,6	-	0,6	0,6	-	-	1,4	0,3	0,6	-	0,3	0,3
		Muscovite+Chlorite in rock fragment	-	-	-	-	-	-	-	-	0,3	-	-	-	-	-	-	-	-	-	-	-	-	-	-	-	-	-
		Heavy mineral single crystal (unspecified)	-	0,3	-	-	-	0,3	0,6	-	-	-	0,3	-	-	0,3	0,3	-	-	-	-	-	-	-	-	-	-	-
		Heavy mineral in rock fragment (unspecified)	-	-	-	-	-	-	-	-	-	-	-	-	-	0,3	-	-	-	-	-	-	-	-	-	-	-	-
		Fe-oxide	0,6	-	0,3	-	-	0,3	0,9	0,6	0,3	-	0,6	-	-	-	-	-	0,6	-	-	-	-	-	-	1,2	-	-
CE	C	Calcite single crystal	12,7	11,7	9,4	11,6	12,7	14,7	15,0	13,1	16,5	15,0	13,1	11,6	15,8	16,3	10,4	12,1	14,5	16,4	10,6	14,2	19,6	18,7	19,3	20,4	21,5	18,1
		Sparitic limestone	13,3	6,3	4,9	3,8	4,7	1,2	5,7	4,7	4,3	5,2	2,5	5,3	8,8	5,1	7,0	4,2	9,5	5,5	15,8	9,3	6,0	5,5	8,1	7,3	8,1	12,8
		Silty-arenitic limestone	-	-	-	2,5	2,2	-	-	-	-	-	4,0	1,9	-	4,8	-	1,4	-	1,1	-	-	2,3	2,9	4,3	7,0	1,7	-
		Mudstone-Wackestone	8,4	11,7	15,8	12,9	13,0	12,8	11,4	12,8	10,1	7,4	11,5	10,7	21,5	15,7	10,7	13,5	16,9	13,2	11,9	16,6	17,6	20,7	20,5	17,0	15,4	17,8
		Bioclast (terrigenous)	0,6		0,6	0,6	0,9	0,9	-	0,3	0,3	0,3	0,6	0,3	2,4	3,8	4,6	3,1	2,1	3,2	3,6	4,5	3,1	2,0	2,0	2,7	3,5	2,2
NCI		Brick and pottery fragments	0,9	0,3	0,6	0,3	-	-	-	-	0,3	0,3	0,3	-	1,5	1,9	1,4	2,2	1,5	2,0	1,2	0,9	1,7	1,7	1,4	1,2	0,6	1,2
CI		Bioclast (penecontemporaneous)	-	-	-	-	-	-	-	-	-	-	-	-	-	-	-	-	-	-	-	0,3	-	0,6	-	-	-	-
		Caliche	-	-	-	-	0,3	-	-	-	-	-	0,3	0,6	-	-	-	-	-	-	-	-	-	-	-	-	-	-
		Undetermined	-	-	-	0,3	-	0,3	-	-	-	-	-	0,3	-	-	-	0,6	-	0,3	-	-	-	-	-	-	-	-
		Total	100,0	100,0	100,0	100,0	100,0	100,0	100,0	100,0	100,0	100,0	100,0	100,0	100,0	100,0	100,0	100,0	100,0	100,0	100,0	100,0	100,0	100,0	100,0	100,0	100,0	100,0

			Tiepido				Nizzola	Guerro				Panaro															
			Modern				*Modern*	*Modern*				*Modern*									*Holocene*				*Late Pleistocene*		
		Sample	T 5	T 7	T 8	T 9	N 1	GU 1	GU 2	GU 3	GU 4	P 11	P 12	P A	P C	P 4	P 7	P 8	P 9	P 10	S 1	S 2	S 3	S 4	S 8	S 12	S 11
NCE	Q	Quartz single crystal	10,4	8,8	11,9	7,3	22,7	8,4	11,7	8,4	10,7	9,6	12,9	13,2	11,7	12,3	12,6	12,3	14,9	14,6	10,3	11,3	13,5	12,2	12,8	18,0	12,1
		Quartz polycrystalline coarse texture	1,5	2,5	2,7	1,5	4,0	0,9	1,8	3,1	2,2	2,8	3,4	2,5	1,6	2,4	4,9	3,8	1,6	3,5	1,8	1,3	0,3	-	3,4	1,2	5,1
		Quartz polycrystalline fine texture	0,3	1,0	1,2	0,6	1,2	1,8	0,3	0,6	1,9	1,2	0,3	1,9	1,9	1,5	0,6	0,9	0,6	1,3	0,3	1,3	1,5	3,3	1,1	1,5	0,6
		Chert	0,3	0,2	-	0,6	0,3	1,8	1,5	0,3	0,6		0,6	0,9	0,9	0,3	0,6	0,9	0,6	0,6	0,6	0,3	0,3	0,7	0,6	0,3	0,6
		Quartz in plutonic-gneissic rock fragment	0,9	1,0	0,6	1,2	1,2	0,3	0,3	0,9	0,6	0,9	2,1	1,3	0,9	0,6	1,5	0,9	0,6	0,9	0,6	0,3	1,5	1,3	2,5	0,6	0,6
		Quartz in metamorphic rock fragment	0,3	0,2	-	-	1,8	-	-	-	-	0,3	-	-	0,3	-	0,3	-	-	0,3	0,3	-	0,6	-	0,3	-	-
		Quartz in volcanic rock fragment	-	-	-	-	-	-	-	-	-	-	-	-	-	-	-	-	-	-	-	-	-	-	-	-	-
		Quartz in clastic rock fragment	1,2	1,5	1,2	4,1	0,3	3,9	1,5	1,3	2,2	2,5	2,1	0,9	1,9	3,0	2,8	0,6	2,2	0,6	2,4	0,3	0,3	-	2,5	3,2	0,6
	K	K-feldspar single crystal	1,8	2,7	3,3	3,2	6,1	2,4	4,9	2,2	2,2	5,9	7,4	4,7	3,2	5,7	6,2	6,0	6,8	5,4	3,0	2,6	2,1	2,0	6,7	5,9	7,0
		K-feldspar in plutonic-gneissic rock fragment		0,2	0,3	0,3	0,3	1,5	-	-	-	-	-	0,3	-	0,6	1,2	0,3	0,6	0,6	1,2	-	0,6	-	0,8	0,9	0,6
		K-feldspar in metamorphic rock fragment	-	-	-	-	-	-	-	-	-	-	-	-	-	-	-	-	-	-	-	-	-	-	-	-	-
		K-feldspar in volcanic rock fragment	-	-	-	-	-	-	-	-	-	-	-	-	-	-	-	-	-	-	-	-	-	-	-	-	-
		K-feldspar in clastic rock fragment	-	-	0,3	-	-	0,6	0,3	-	-	0,3	-	-	0,3	0,6	-	0,9	0,6	0,6	0,6	0,3	-	-	-	0,3	0,3
	P	Plagioclase single crystal	4,6	3,9	4,6	3,5	4,6	2,4	1,8	4,1	5,3	3,7	9,2	7,2	7,6	5,1	5,8	4,7	4,7	5,1	7,0	6,8	5,2	7,6	8,1	8,3	8,3
		Plagioclase in plutonic-gneissic rock fragment	-	-	-	0,9	-	-	0,3	0,6	-	-	0,9	1,3	0,3	1,2	0,3	0,6	-	-	0,6	0,3	1,8	1,3	1,1	1,2	1,6
		Plagioclase in metamorphic rock fragment	-	-	-	-	-	-	-	-	-	-	-	-	-	-	-	-	-	-	-	-	-	-	-	-	-
		Plagioclase in volcanic rock fragment	-	-	-	-	-	-	-	-	-	-	-	-	-	-	-	-	-	-	-	-	-	-	-	-	-
		Plagioclase in clastic rock fragment	0,3	0,2	-	0,3	0,3	-	-	-	0,9	0,3	0,6	1,6	0,6	0,3	-	-	-	-	0,6	0,6	0,6	0,3	0,3	1,8	-
	L	Metamorphic rock fragment	-	-	0,3	-	-	-	-	-	-	-	-	0,9	0,6	-	-	-	-	0,6	0,3	-	-	0,3	-	0,3	-
		Volcanic rock fragment	-	-	-	-	-	-	-	-	-	-	-	-	-	-	-	-	-	-	-	-	-	-	-	-	-
		Hypoabyssal lithic	-	-	-	-	-	-	-	-	-	-	-	0,3	-	-	-	-	-	-	-	-	-	-	-	-	-
		Spilite	-	-	0,3	-	-	-	0,3	-	0,3	0,6	-	-	0,3	-	0,3	0,3	-	0,3	-	-	0,3	-	0,3	0,9	-
		Serpentinite	0,9	1,0	0,6	0,3	-	-	-	-	-	0,6	1,2	1,6	0,6	0,6		0,9	0,9	0,3	0,6	-	0,3	-	0,8	1,2	1,0
		Clastic lithic Shale	6,4	6,4	7,0	8,4	8,0	3,3	5,8	9,1	6,6	19,8	14,1	8,5	16,1	18,9	11,4	13,2	13,4	12,7	11,9	18,0	11,3	14,8	17,3	18,3	15,6
		Siltstone	9,2	9,1	10,3	10,2	16,9	13,1	9,5	10,6	7,5	12,4	10,4	13,8	10,4	9,0	10,5	14,2	8,4	11,4	14,3	14,5	14,4	12,8	14,5	9,4	15,3
	M	Muscovite+Chlorite single crystal	0,3	-	-	0,6	-	0,6	0,3	0,9	-	0,3	0,6	-	0,9	1,2	0,6	-	0,6	0,3	-	-	-	-	0,6	-	-
		Muscovite+Chlorite in rock fragment	-	-	-	-	-	-	-	-	-	-	-	-	-	-	-	-	-	-	-	-	-	-	-	-	-
		Heavy mineral single crystal (unspecified)	0,3	0,2	-	0,3	0,3	0,3	-	-	-	-	-	-	-	-	-	-	-	-	-	-	-	-	-	-	-
		Heavy mineral in rock fragment (unspecified)	-	-	-	-	-	-	-	-	-	-	-	0,3	-	-	-	-	-	-	-	-	-	-	-	-	-
		Fe-oxide	0,6	-	1,5	-	-	-	1,2	0,9	0,6	0,6	0,3	0,3	-	-	-	-	-	-	-	0,3	-	0,3	-	-	-
CE	C	Calcite single crystal	28,2	24,6	21,0	23,5	7,7	24,2	23,9	26,6	26,7	14,2	13,2	15,4	12,3	9,9	16,3	17,3	18,0	15,5	13,7	17,4	14,4	16,8	13,1	9,7	14,6
		Sparitic limestone	9,8	13,8	13,1	9,9	4,0	20,6	15,6	14,1	14,8	7,7	6,4	3,8	5,4	7,2	10,8	5,7	7,1	7,3	5,5	2,6	6,4	5,9	5,6	4,7	4,8
		Silty-arenitic limestone	4,6	-	-	2,6	-	-	-	-	-	-	-	3,1	3,8	-	-	-	-	-	3,6	1,9	4,6	4,9	-	2,4	-
		Mudstone-Wackestone	14,1	19,7	15,2	18,9	16,9	12,5	16,3	15,0	16,0	14,2	13,5	13,8	16,1	17,4	12,9	15,1	16,8	17,7	18,2	16,4	17,7	13,2	7,3	9,4	11,1
		Bioclast (terrigenous)	2,1	1,0	3,0	2,0	-	0,3	0,9	0,3	-	1,2	0,6	0,6	1,6	1,8	0,3	0,6	1,2	0,3	-	1,3	0,6	0,3	0,3	0,6	-
NCI		Brick and pottery fragments	0,9	2,0	0,9	-	2,8	1,2	1,5	0,6	0,6	0,3	-	0,9	-	0,6		0,6	0,3	-	0,6	-	0,6	2,0	-	-	-
CI		Bioclast (penecontemporaneous)	0,6	-	-	-	-	-	-	-	-	0,3	-	0,6	-	-	-	-	-	-	-	-	-	-	-	-	-
		Caliche	-	-	-	-	-	-	-	-	-	-	-	-	-	-	-	-	-	-	1,5	2,3	0,9	-	-	-	-
		Undetermined	-	-	0,6	-	0,6	-	-	0,3	-	-	-	0,3	0,3	-	-	-	-	-	0,3	-	-	-	-	-	-
		Total	100,0	100,0	100,0	100,0	100,0	100,0	100,0	100,0	100,0	100,0	100,0	100,0	100,0	100,0	100,0	100,0	100,0	100,0	100,0	100,0	100,0	100,0	100,0	100,0	100,0

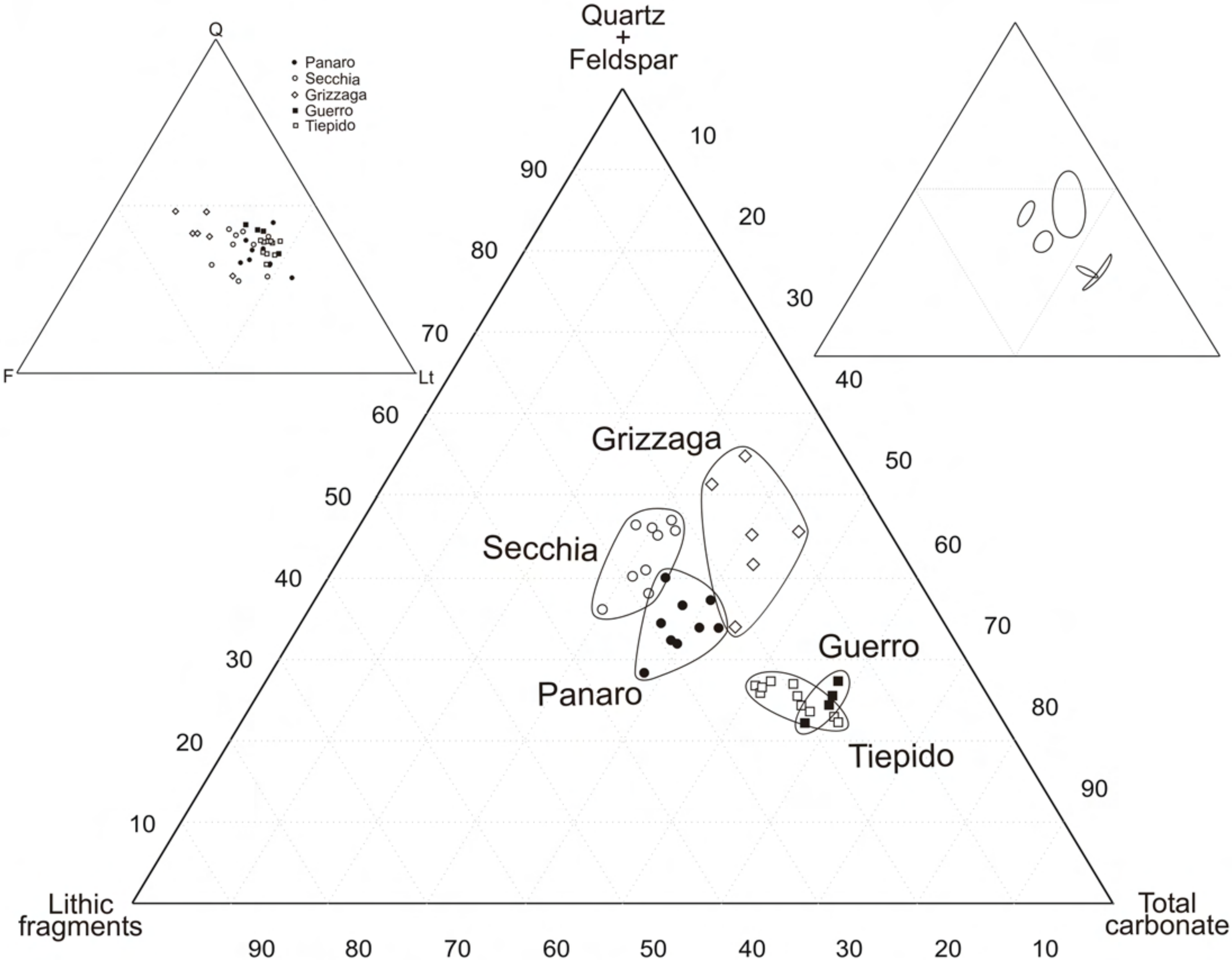

Q
F
Lt
Panaro
Secchia
Grizzaga
Guerro
Tiepido
Quartz
+
Feldspar
Lithic
fragments
Total
carbonate
Grizzaga
Secchia
Panaro
Guerro
Tiepido
90
80
70
60
50
40
30
20
10

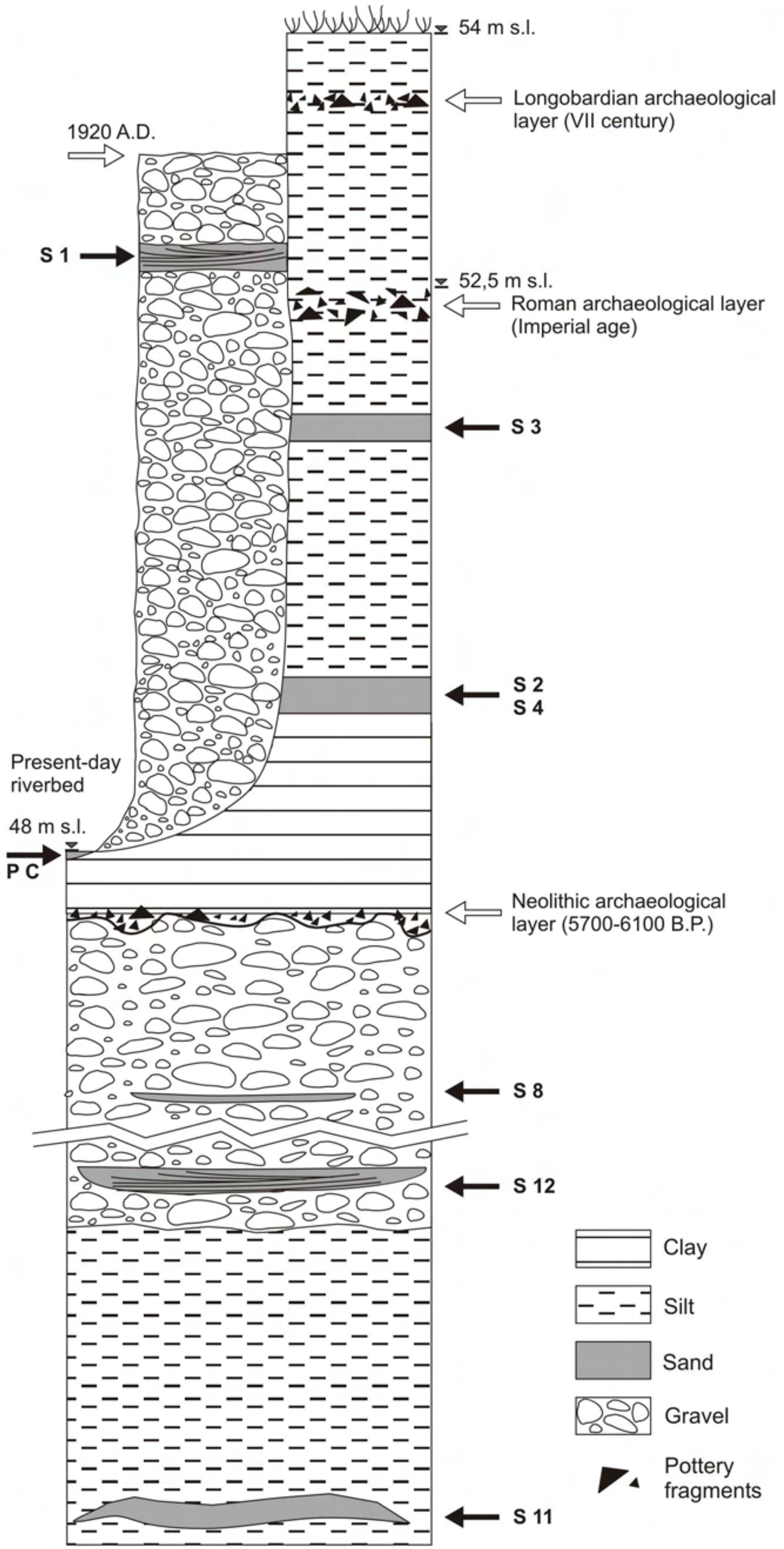

54 m s.l.
Longobardian archaeological layer (VII century)
1920 A.D.
S 1
52,5 m s.l.
Roman archaeological layer (Imperial age)
S 3
S 2
S 4
Present-day riverbed
48 m s.l.
P C
Neolithic archaeological layer (5700-6100 B.P.)
S 8
S 12
Clay
Silt
Sand
Gravel
Pottery fragments
S 11

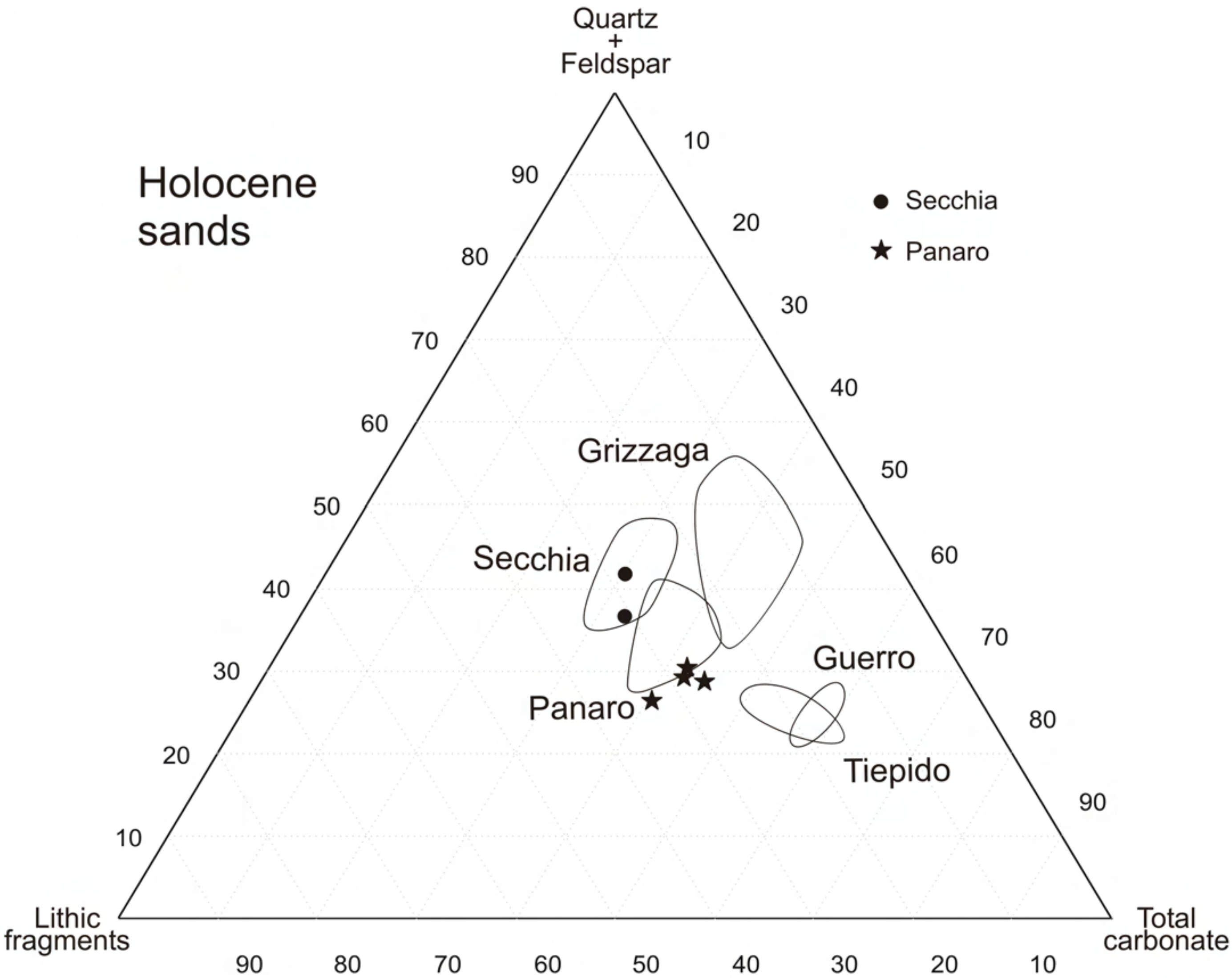

Holocene
sands
Quartz
+
Feldspar
Lithic
fragments
Total
carbonate
Secchia
Panaro
Grizzaga
Secchia
Panaro
Guerro
Tiepido
90
80
70
60
50
40
30
20
10
10
20
30
40
50
60
70
80
90
90
80
70
60
50
40
30
20
10

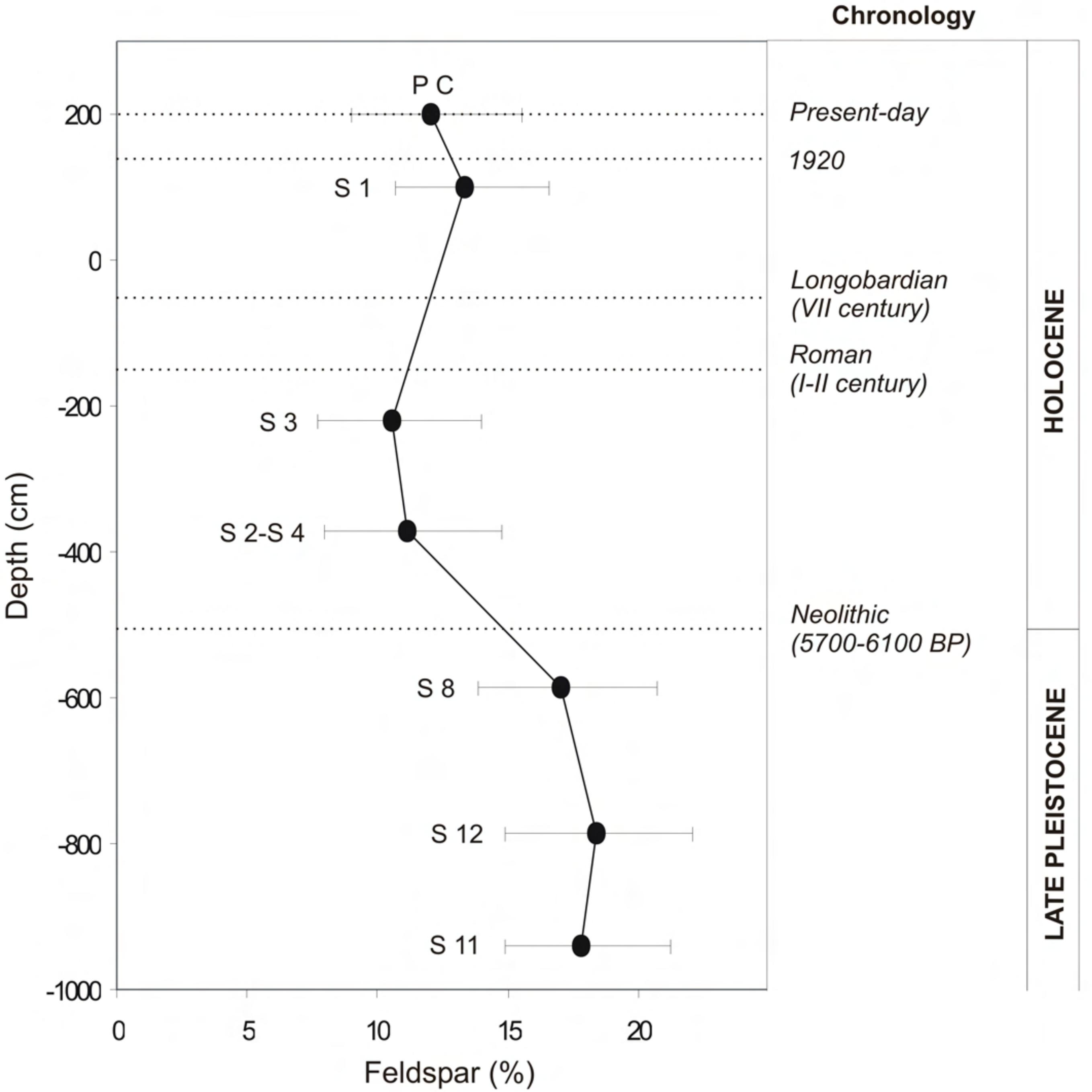

Chronology
P C
Present-day
1920
S 1
Longobardian
(VII century)
Roman
(I-II century)
S 3
S 2-S 4
Neolithic
(5700-6100 BP)
S 8
S 12
S 11
HOLOCENE
LATE PLEISTOCENE
Depth (cm)
200
0
-200
-400
-600
-800
-1000
0
5
10
15
20
Feldspar (%)

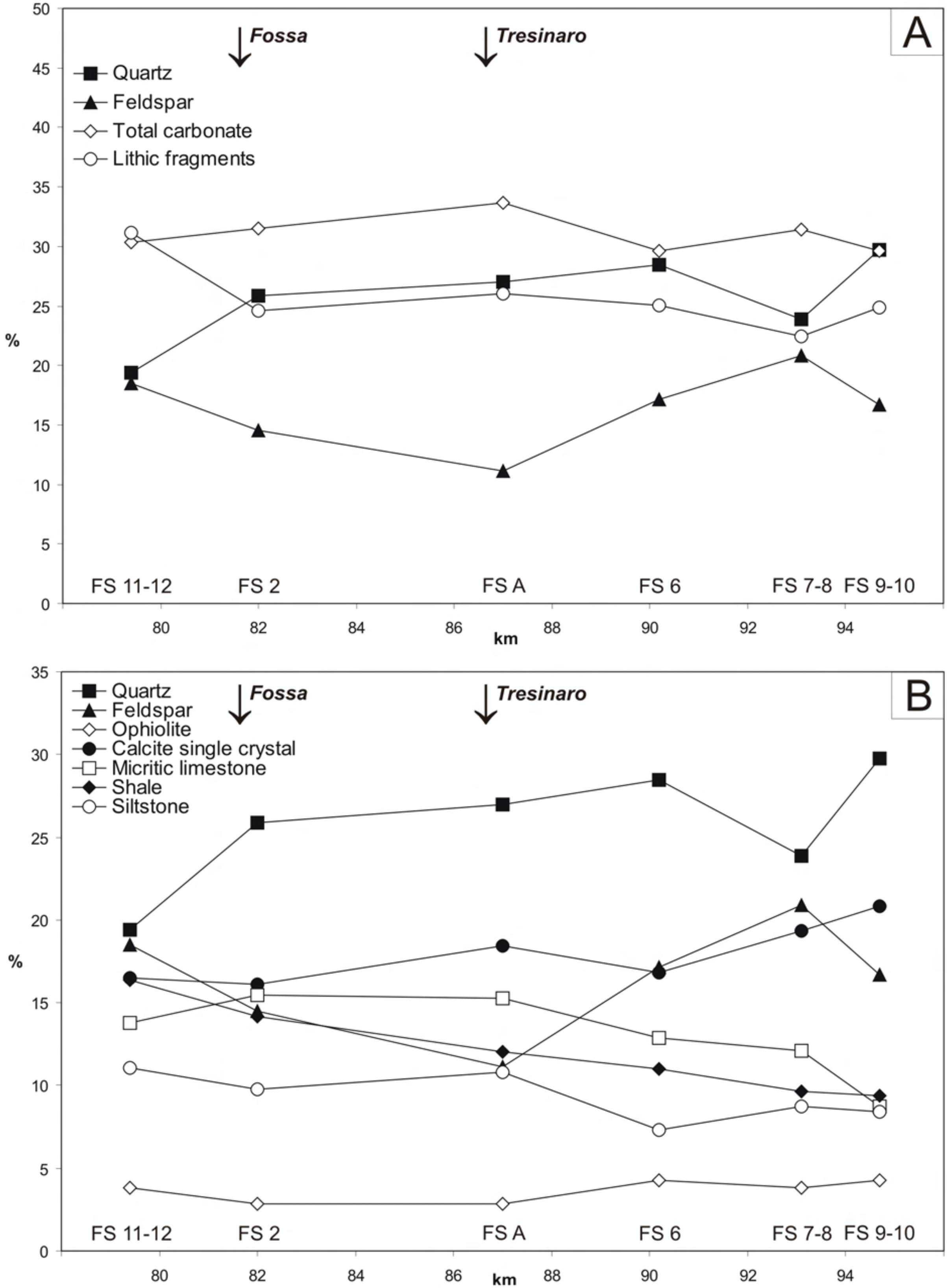
A
Fossa
Tresinaro
Quartz
Feldspar
Total carbonate
Lithic fragments
%
FS 11-12
FS 2
FS A
FS 6
FS 7-8
FS 9-10
km
B
Quartz
Feldspar
Ophiolite
Calcite single crystal
Micritic limestone
Shale
Siltstone

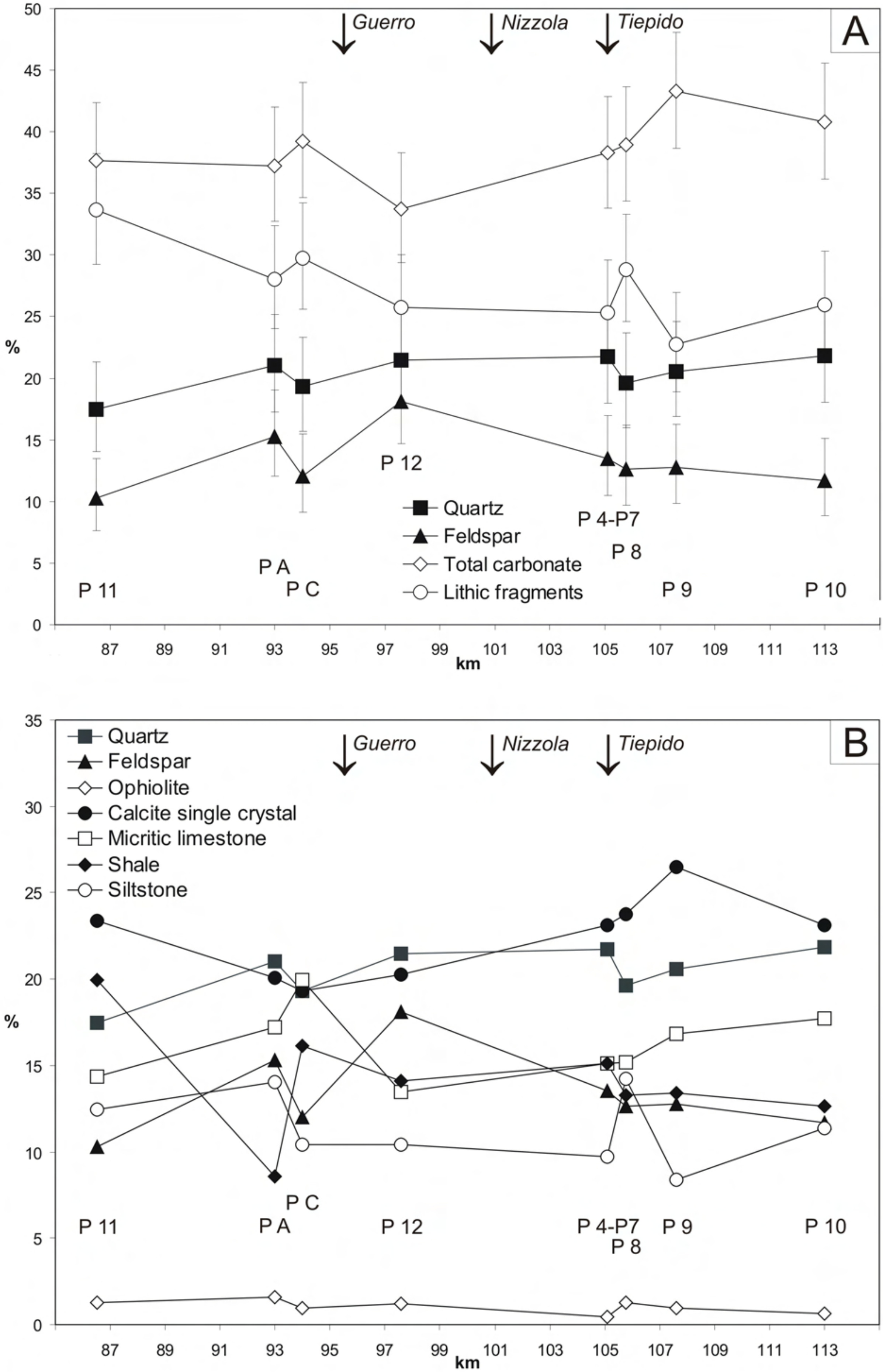
A
Guerro
Nizzola
Tiepido
Quartz
Feldspar
Total carbonate
Lithic fragments
P 11
P A
P C
P 12
P 4-P7
P 8
P 9
P 10
%
km
B
Quartz
Feldspar
Ophiolite
Calcite single crystal
Micritic limestone
Shale
Siltstone

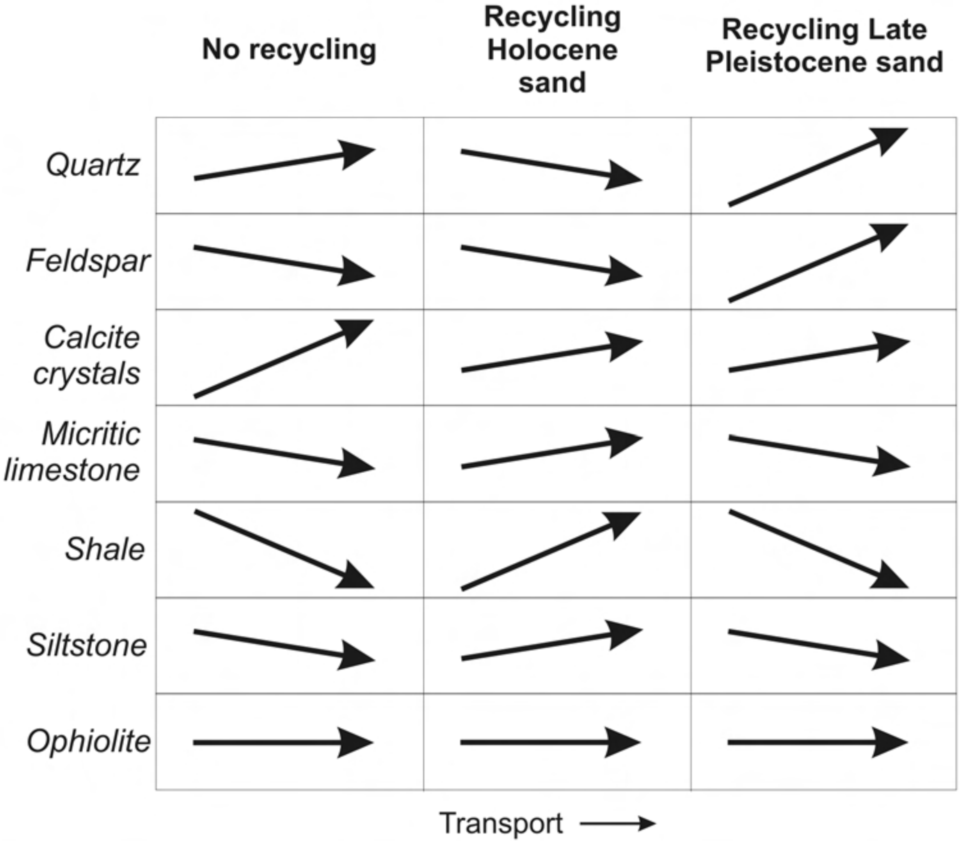
No recycling
Recycling Holocene sand
Recycling Late Pleistocene sand
Quartz
Feldspar
Calcite crystals
Micritic limestone
Shale
Siltstone
Ophiolite
Transport